Available online at www.sciencedirect.com
SCIENCE DIRECT
Polymer 46 (2005) 3307–3317
polymer
www.elsevier.com/locate/polymer

Introducing open films of nanosized cellulose—atomic force microscopy and quantification of morphology

E. Kontturi[a,*], P.C. Thüne[a], A. Alexeev[b], J.W. Niemantsverdriet[a]

[a]*Schuit Institute of Catalysis, Eindhoven University of Technology, P.O. Box 513, 5600 MB Eindhoven, The Netherlands*
[b]*Laboratory of Macromolecular Chemistry and Nanoscience, Eindhoven University of Technology, P.O. Box 513, 5600 MB, Eindhoven, The Netherlands*

Received 17 August 2004; received in revised form 16 December 2004; accepted 14 February 2005
Available online 24 March 2005

Abstract

A method for preparing open, sub-monolayer cellulose films on a silicon substrate is introduced, and the open films were quantified using the three-dimensional information from atomic force microscopy (AFM) height images. The preparation method is based on spin coating low concentrations of trimethylsilyl cellulose (TMSC) on silicon and hydrolysing the TMSC to cellulose using a vapour phase acid hydrolysis. AFM showed that the surfaces consist of nanosized cellulose patches which are roughly 50–100 nm long, 20 nm wide, and 1 nm high. The volume of the cellulose patches was quantified. Examination of the cross section of the cellulose patches revealed that the exaggeration of the lateral dimensions by the AFM tip is small enough to account for a mere $\pm 2\%$ error in the volume quantification. Pilot experiments showed that the volume of the cellulose was largely restored in a wetting/drying cycle but the morphology changed considerably. Because of their small size, the cellulose patches provide a novel approach for interpretation on the molecular architecture of cellulose.

Keywords: Atomic force microscopy; Cellulose model surface; Open film

1. Introduction

As the most abundant biopolymer, cellulose is widely available in nature for commercial use. Applications in, for instance, paper and textile industry are numerous, and cellulose has been subject to extensive research throughout the past century. A complete supramolecular description was under scrutiny for nearly 100 years [1], but recently, the two crystalline allomorphs of native cellulose (cellulose I_α and I_β) have been resolved [2,3]. However, much remains unknown, for instance, the possible ordering in amorphous cellulose and its rearrangements during wetting and subsequent drying [4–6]. The lack of information provides a hindrance while interpreting the molecular level phenomena that take place during industrial processing of cellulose, for example, interactions with water.

Native cellulose is usually included in a cell–wall matrix like wood fibre. This means not only that other compounds are embedded in cellulose but that native cellulose comes in both amorphous and crystalline forms [7]. Furthermore, each individual cell is different in morphology and chemical composition. Under these circumstances, a need for a representative model of cellulose is evident.

Smooth, ultra-thin model surfaces of well-defined substances provide means to observe the chemical and morphological changes in various conditions that often resemble industrial processes. The amount of fundamental information that can be extracted from model surfaces is already widely recognized in, for instance, catalysis research [8] and polymer technology [9]. The first successful model surface of cellulose was introduced a decade ago when Langmuir–Blodgett (LB) deposition was used to produce films of trimethylsilyl cellulose (TMSC) which could be easily hydrolysed to cellulose [10,11]. Recently, spin coating has also emerged as a method for cellulose model surface preparation [12,13]. The applications of these model surfaces have, however, been restricted mainly to the adsorption behaviour of polyelectrolytes on cellulose films [14,15] or the interactions between two cellulose surfaces in the presence of polyelectrolytes [16]. In this paper, we explore and establish a different approach: we will introduce a new type of cellulose surface consisting of nanosized

* Corresponding author. Tel.: +31 40 2473068; fax: +31 40 2473481.
E-mail address: e.j.kontturi@tue.nl (E. Kontturi).

0032-3861/$ - see front matter © 2005 Elsevier Ltd. All rights reserved.
doi:10.1016/j.polymer.2005.02.087

domains which appear more distinctly when characterised by atomic force microscopy (AFM). The applicability of these films is further demonstrated by following a wetting/drying process with water.

In previous work, this group has introduced a simplified method to prepare model surfaces of cellulose by spin coating TMSC on silicon and transferring it to cellulose with an acid hydrolysis [17,18]. The preparation process thus combined the advantages of LB-method and spin coating (Scheme 1). This method yields thin (ca. 20 nm) layers of cellulose with a roughness variation of max. 3 nm. It is efficient in speed and reproducibility.

Although long since recognized as an effortless coating technique for thin films [19], spin coating has recently gained status as a method to prepare well-ordered structures with small loadings [20,21]. Inorganic, small molecular weight compounds arrange in so-called open films when the concentration of coating solution is made so low that a coverage smaller than monolayer is produced. These structures can arrange into aggregates which resemble islands of the coated material on a flat substrate [22], or, as is often the case in polymer chemistry, open films are used to study evenly spread single molecules with AFM [23,24]. Applications of the films from single polymer molecules include determining the molecular weight distribution [25] and visualising the phase transition during lateral compression [26]. We set out to investigate whether any kind of open films are feasible with cellulose using the previously published method. With a significant reduction of the TMSC concentration in spin coating, we have achieved open films of cellulose which are somewhat reminiscent of fibres in a miniature scale. These patches of cellulose are implanted on a silicon wafer. To our knowledge, the nearest account to open films of cellulose in the literature appeared when Kasai et al. managed to successfully prepare honeycomb-patterned cellulose films, regenerating the cellulose from a cellulose acetate film [27]. Strictly speaking, these films were not open films because they possessed a closed cellulose layer between the conspicuous honeycomb structures. Our open films are, in any case, very different. The honeycomb-patterned films are a continuous network of cellulose with pore-sizes running up to several tens of micrometers, whereas our TMSC based open films consist of nanosized patches of cellulose with at most a few tens of nanometres between them. The open films introduced in this paper offer possibilities for nano-scale interpretation of the behaviour of cellulose.

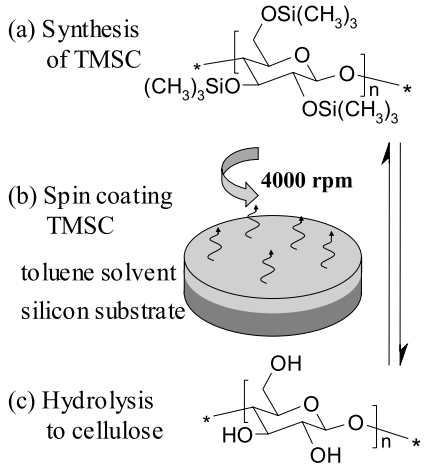

Scheme 1.

Because of the 'open' nature of the films, the cellulose patches are conspicuous on the smooth silicon substrate in AFM analysis, even when regarding the small size of the patches. On the other hand, their small size enables interpretation on the supramolecular chemistry of cellulose, which is different from the morphological interpretation of the closed films. We also want to point out that AFM is not merely an imaging technique; three-dimensional data provides a lot of quantitative information. As an example, we evaluate the volume of the cellulose patches on silicon.

As a pilot experiment for applications, we have used the open films to examine rearrangements in cellulose during wetting and drying. Such rearrangements may also occur in natural fibres during paper recycling: wetting and subsequent drying decreases the strength properties of fibres and this quality decrease is still not understood fundamentally [28,29]. We have to emphasize, however, that the native cellulose matrix differs a great deal from the model surfaces of pure cellulose on a silicon substrate.

Research on cellulose model surfaces with wetting/drying is not unique. Fält et al. have already investigated the swelling behaviour of closed cellulose films of various charge densities with a quartz crystal microbalance [30]. Our approach, however, is different. We examine the swelling and shrinking of small scale cellulose features with AFM, i.e. visualise the morphology during the rearrangements.

2. Experimental

Materials. Microgranular cellulose was purchased from Sigma. Dimethylacetamide (DMAc), lithium chloride (LiCl), hexamethyldisilazane (HMDS), methanol, and tetrahydrofuran (THF) were all analytical (p.a.) grade from Aldrich. Distilled water and nitrogen of purity grade 5 were used.

Preparation of trimethylsilyl cellulose (TMSC) (Scheme 1(a)). 2 g of microgranular cellulose was dissolved to lithium chloride (9% w/v) in 200 ml dimethylacetamide (DMAc/LiCl) as described elsewhere [31]. After the cellulose had completely dissolved, the solution was heated to 80 °C in water bath and 20 ml of HMDS was added in a steady flow within 1 h in a nitrogen atmosphere. The mixture was cooled down and some methanol was added to enhance the precipitation of TMSC which was left to proceed overnight. The precipitated TMSC was filtered and

dissolved into 80 ml THF and re-crystallised in 1000 ml of methanol. After filtration, the re-crystallised TMSC was washed several times with methanol and dried in a vacuum desiccator. Besides the characteristic cellulose spectrum, the final product yielded distinct infrared peaks at 1251 (δ Si–C) and 842 (ν Si–C) cm^{-1} which were in correlation with literature Ref. [32]. Extensive characterization of the TMSC prepared in our laboratory has been published earlier in Ref. [18].

Preparation of model surfaces (Scheme 1(b)). The TMSC was dissolved in toluene up to solution concentrations of 10, 20 or 50 mg/l and 10 g/l. The solutions were spin coated with a spinning speed of 4000 revolutions per minute (rpm). The substrates used were untreated silicon wafers (Topsil) with (100) surface orientation, cut to ca. 2×2 cm^2 squares.

The regeneration of the spin coated TMSC (Scheme 1(c)) was performed by acid hydrolysis. A small amount of 2 M hydrochloric acid was placed on the bottom of a glass container with a holder for the spin coated wafers. The vapour pressure was allowed to stabilise for 1 h, after which the wafer was placed in the container and the vapour phase acid hydrolysis was carried out for 2 min.

Atomic force microscopy (AFM) was performed with Solver P47H base with a SMENA head, manufactured by NT-MDT. The cantilever of choice was contact silicon CSC12 manufactured by Micromasch, used in tapping mode. The typical force constant of the cantilever was in the region of 2.0 N/m and the typical resonance frequency around 150 kHz. Radius of curvature for the tip was always less than 10 nm. Free oscillating amplitude of the cantilever was approximately 10 nm, and the set point amplitude was set close (~70%) to the free-oscillating amplitude in order to work in the regime where long range attractive forces dominate the amplitude reduction. This gave the best topographic information and minimised the sample indentation [33,34]. To prevent the broadening of the tip curvature radius by tip contamination, we replaced the tip each time a hint of contamination became apparent, such us a double tip or increase in width with the more recently scanned patches. Since flawless phase imaging was exceptionally difficult even after refined set point adjustment, all images presented are amplitude images, unless otherwise mentioned. All presented quantitative data is extracted from height images. All measurements were performed at room temperature.

Volume quantification. In an AFM image, each pixel has a height which contributes as one height count to the height distribution. Fig. 1(a) shows the histogram of the distribution of height counts from the height image of one of the article's AFM images, namely Fig. 2(c). The histogram can be resolved into two peaks by a Gaussian fit reasonably well ($R^2=0.9985$).

The two Gaussian peaks in Fig. 1(a) represent the silicon substrate and the cellulose nanopatches. Areas of the silicon peak and the cellulose peak divided by the total area give the uncovered fraction of silicon (θ_{Si}) and the coverage of cellulose (θ_{cell}), respectively. Full width at half height of the

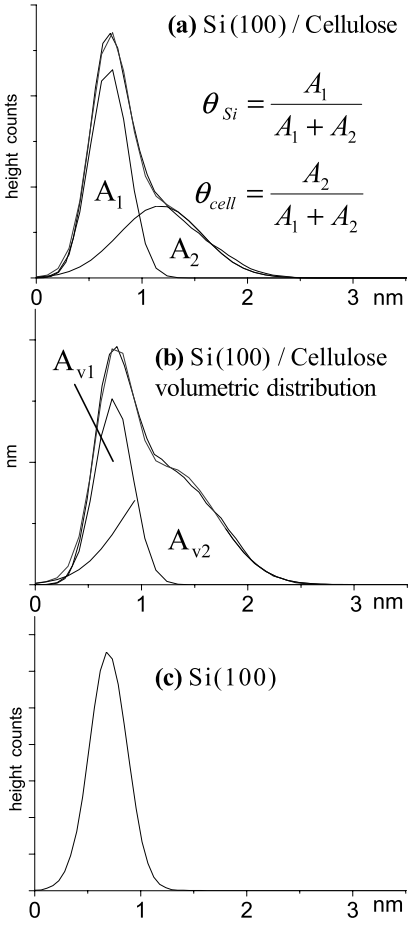

Fig. 1. Distributions of height counts of 1×1 μm^2 AFM scans: (a) height distribution of an open cellulose film spin coated from 20 mg/l TMSC solution (from Fig. 2(c)), resolved into A_1, the height counts of the silicon between the cellulose patches, and A_2, the height counts from the cellulose patches; (b) volumetric height distribution, acquired by multiplying height counts of (a) by their height, A_{V1} is the artificial volume of silicon between the cellulose and A_{V2} is the volume of the cellulose patches, including the volume of silicon under them; (c) height distribution of a plain silicon wafer (to be compared with A_1). θ_{Si} and θ_{cell} refer to the uncovered fraction of silicon and the coverage of cellulose in the open films, respectively.

silicon peak corresponds to the roughness of the silicon substrate, 0.36 nm in Fig. 1(a). This number is in accordance with AFM measurements which we performed with uncoated, untreated silicon wafers (Fig. 1(c)). Although the wafer surface is initially that of a smooth single crystal, silicon between the cellulose patches has an artificial volume A_{V1}. This silicon volume arises because the height of the silicon surface is not zero. The lowest measured height is set at zero.

To determine the volume, it is not the height distribution graph itself but a graph where the height counts are multiplied by their height (Fig. 1(b)), that has to be integrated. We have named this graph the volumetric height distribution; its area ($A_{V1}+A_{V2}$) corresponds to the apparent volume of the whole 1×1 μm^2 AFM scan (unit: $nm^2\times$ [dimensionless pixel]). Since the silicon under the cellulose also has an artificial volume, it prevents us from simply

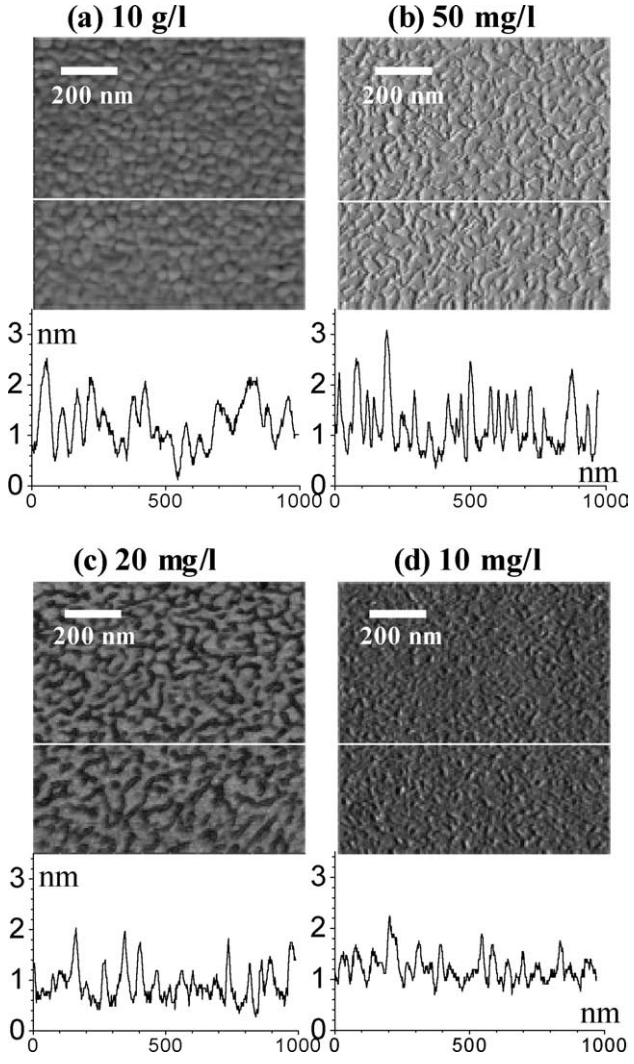

Fig. 2. AFM images of cellulose films, 1×1 μm^2 scans: (a) closed film with thickness of 18 nm spin coated from 10 g/l TMSC solution, (b) open film spin coated from 50 mg/l TMSC solution, (c) open film spin coated from 20 mg/l TMSC solution, (d) open film spin coated from 10 mg/l TMSC solution. Hydrolysed to cellulose with 2 M HCl vapour for 2 min. A representative height scan marked in the image is presented under each image.

integrating the A_{V2} area and regarding it as the volume of the cellulose. The volume of the silicon between the cellulose and the silicon under the cellulose (A_{V1}/θ_{Si}) has to be substracted from the total volume ($A_{V1}+A_{V2}$):

$$V_{cell} = \left(A_{V1} + A_{V2} - \frac{A_{V1}}{\theta_{Si}}\right)\frac{A_{pix}}{l_h} \quad (1)$$

where A_{V2} is the volume of the cellulose with silicon under it (Fig. 1(b)), A_{V1} is the artificial volume of the silicon between the cellulose patches (Fig. 1(b)), and θ_{Si} is the coverage of silicon on the surface (Fig. 1(a)). The dimensions are corrected with A_{pix}, the area of one pixel having one height count (1000×1000 nm^2/(512×512) = 3.8 nm^2), and l_h, the height step, i.e. resolution of the height, parameter of the AFM (0.07 nm in our case). The total artificial volume of the silicon (A_{V1}/θ_{Si}) is evaluated under the presumption that the silicon under the cellulose has the same height distribution as the visible silicon.

Chemical analysis of the open film was omitted. The closed films prepared in our laboratory were already extensively analysed in Ref. [18], and there is no reason to believe that the open surfaces, which were prepared by the same person in exactly the same way except for the smaller amount of TMSC, should differ in chemical composition, i.e. that the hydrolysis of TMSC to cellulose (Scheme 1(c)) is not complete. In order to be sure of the extent of hydrolysis, the hydrolysis time was doubled to 2 min. Thicker films were characterised with X-ray photoelectron spectroscopy (XPS) and attenuated total reflectance infrared spectroscopy (ATR-IR) [18]. The open surfaces caused a problem in the XPS, since the pivotal carbon peak was blurred by omnipresent hydrocarbon impurities, usually originating from the XPS equipment itself. In addition, the detection limit of the ATR-IR was not enough for the open surfaces. In other words, the amounts of cellulose in the sub-monolayer open films were too small to be analysed properly with these techniques. Work is currently under progress to find a technique applicable to our surfaces but it is beyond the scope of this introduction.

3. Results and discussion

3.1. Introducing the cellulose patches

Generally speaking, if the concentration of the spin coating solution is so low that there is not enough coating substance to form a closed film, a uniform sub-monolayer coverage is formed, or the substance arranges itself into isolated structures, islands, on the flat substrate. The idea of our study was to examine if a drastic decrease of TMSC concentration in spin coating had a similar effect on our cellulose films, i.e. whether the cellulose, hydrolysed from TMSC, formed islands on the silicon substrate. Fig. 2(a) shows an AFM image of a closed cellulose film with thickness of 18 nm. Empirically, 50 mg/l—1/200 of concentration needed to prepare the 18 nm films—was determined as the point, in which phase separation of silicon and cellulose was starting to show (Fig. 2(b)). Ideal structures were found at 20 mg/l concentration: Fig. 2(c) shows distinct patches of cellulose and flat silicon between the cellulose. The remarkable feature with the cellulose islands in Fig. 2(c) is that, in lateral dimensions, they bear a resemblance to natural fibres with their longitudinal shape (ca. $20\times(50–100)$ nm). The height of the cellulose patches is very small, manual analysis of 10 height scans (ca. 80 patches) gave an average height of 0.9 nm after subtraction of the silicon background. Fig. 2(d) demonstrates that 10 mg/l TMSC coating concentration is not enough to form distinct cellulose patches for the AFM. The cellulose

patches in this case are clearly too small to stand out properly from the roughness of the silicon substrate. Roughness is the reason why films from single polymer molecules cannot usually be distinguished on a silicon substrate and the smoother mica must be applied [24]. This observation encourages the assumption that the patches in Fig. 2(b) and (c) are really agglomerates of several cellulose chains arranged longitudinally and not, for instance, single cellulose molecules whose lateral dimensions have been greatly exaggerated by the AFM tip. Further proof is presented in Section 3.2.

Fig. 3 shows the extraordinary morphological difference between low loading TMSC film and the subsequently hydrolysed cellulose film. Unfortunately the softness of TMSC does not allow high quality AFM imaging, but one can recognize that the TMSC film (Fig. 3(b)) is still a closed film and its roughness follows closely the roughness of the underlying silicon wafer (Fig. 3(a)). The hydrolysis transforms the film completely as the absence of the bulky trimethylsilyl groups and the intermolecular hydrogen bonding of the introduced hydroxyl groups makes the structure more compact. Scratching of the TMSC layer revealed its thickness of 2 nm. The change from a closed 2 nm TMSC film to 0.9 nm cellulose patches with ca. 40% coverage (see Section 3.2) accounts for ca. 80% contraction. Similar phenomenon is observed with closed cellulose films: in the case of 10 g/l TMSC coating, the thickness of the hydrolysed cellulose film is 18 nm as opposed to 45 nm for the corresponding TMSC layer, a 40% decrease in volume [18]. The contrast between the low loading TMSC and open cellulose films is even more drastic, which suggest that the cellulose in the open films has a higher degree of order than in the closed films. When the cellulose is formed from TMSC, it can be voluminous enough to cover the whole surface, but individual cellulose chains prefer not to arrange parallel to each other as a monolayer or a bilayer. Instead, small aggregates of several chains are formed because cellulose chains have more affinity towards each other than the silicon substrate. The arrangement of cellulose chains into the worm-like structures during hydrolysis depends on the original morphology of the TMSC layer, the cellulose–silicon interaction and the cellulose–cellulose interaction. Therefore, the structure of the cellulose domains is likely to be rather different from the structure of cellulose in the cell wall matrix.

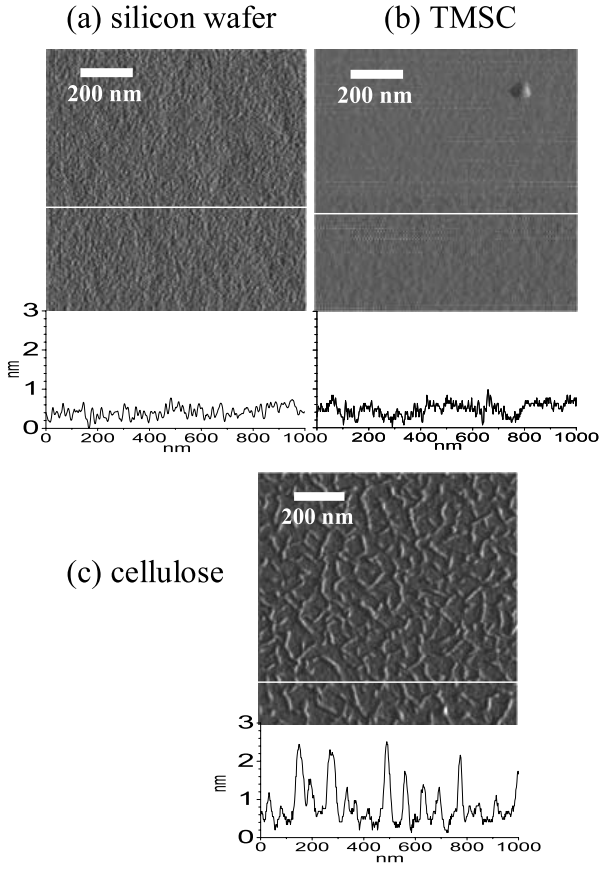

Fig. 3. 1×1 μm^2 AFM images of (a) untreated silicon wafer, (b) TMSC film spin coated from 20 mg/l solution, (c) cellulose film hydrolysed from the TMSC film in (b).

Fig. 4 illustrates a smaller AFM scan (higher magnification) from the sample of Fig. 3(c) (180×180 nm^2). Under scrutiny, the longitudinal cellulose patches appear to be constructed from small grain-like structures, sometimes no more than 10 nm long. The nature of these grains is, in many ways, ambiguous. The closed cellulose films are largely

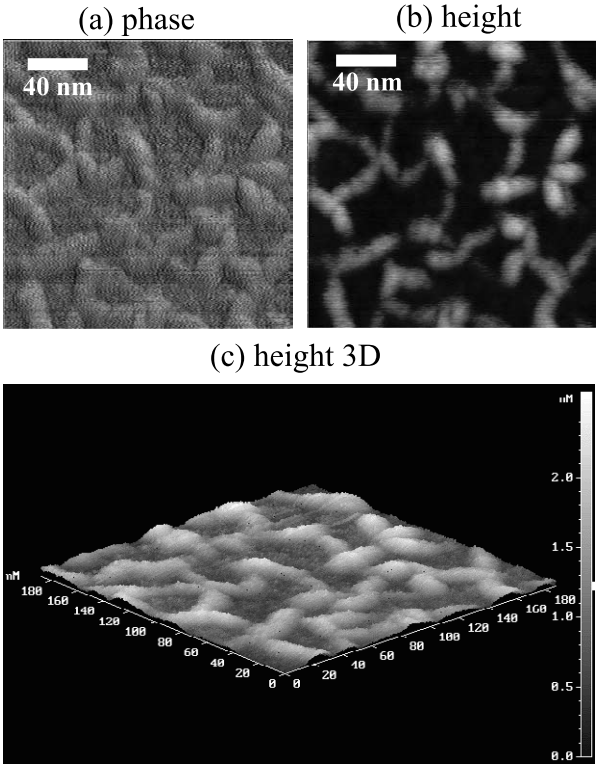

Fig. 4. AFM images of an open cellulose film on silicon, spin coated from 20 mg/l TMSC solution, hydrolysed to cellulose with 10% HCl vapour for 2 min; 180×180 nm^2 scans: (a) phase image, (b) height image, (c) three-dimensional height image.

amorphous, based on the evidence of their IR-data during swelling [18]. We suspect also the open films be mainly amorphous because they swell considerably in water (see Section 3.3). Amorphous cellulose has always been ignored in literature at the expense of crystalline cellulose and accounts of its arrangement are based on speculation rather than on hard evidence. In fact, 'amorphous' is not an explicit term since amorphous cellulose probably possesses order to some extent [35,36]. The grains could emerge from bent or twisted chains but the verification of this would need extensive exploitation of analytical techniques. Moreover, we could speculate that the cellulose patches have a degree of crystallinity—or that they are at least locally ordered—and the grain-like structure is a product of amorphous regions in between the crystalline ones. This kind of supramolecular structure is prevalent in, for instance, wood microfibrils which pass through crystalline regions of ca. 60 nm in length with less ordered amorphous regions between them [37].

3.2. Volume quantification of the cellulose patches

The suitability of the cellulose patches to the volumetric analysis by Eq. (1) and their reproducibility are demonstrated in Table 1. Four surfaces were prepared with TMSC concentration of 20 mg/l, and subsequently hydrolysed to cellulose; thus, similar surfaces as in Fig. 2(c). The surfaces were imaged by AFM on different days with different individual tips. The reproducibility of the surfaces and the volume quantification by Eq. (1) are both remarkable.

The precision of the volumetric determination by Eq. (1) is a result of the distinct dimensions of the cellulose patches. Examining a cross section of a patch, their average height (1 nm) is very small compared with their mean width (20 nm). When a cross section of a patch is fitted with a parabola, comparison with a parabola representing the AFM tip (10 nm radius of curvature) shows that the width of the measured cross section is not exaggerated by more than 2 nm. This means an exaggeration of 8% for the volume quantification.

The tip error in AFM, on the other hand, is caused by varying degrees of lateral exaggeration, i.e. diverse tips. Let us assume that 5 nm is the smallest radius of curvature for the used tips; the comparison with a cross sectional parabola of a cellulose patch yields then a lateral exaggeration of 1 nm in the patch width. This accounts for a 4% exaggeration in the volume quantification by Eq. (1). Therefore, the average exaggeration of the volume quantification is 6% for AFM tips whose radius varies between 5 and 10 nm. The error is $\pm 2\%$. This error is in excellent agreement with Table 1. To maintain such a narrow error margin, care must be taken of the sample indentation and tip contamination, explained in Section 2.

The volume quantification by Eq. (1) was applied to all of the surfaces in Fig. 2 and the results are collected to Table 2. The volume of the closed surface is calculated as a cube with a height of 18 nm (film thickness).

The low tip exaggeration and error in the AFM measurements and the subsequent volume determination are caused by the characteristic dimensions of the cellulose domains. As shown in the next section, the tip error grows considerably when the height of the patches grows. Nevertheless, the ease of reliable volume determination is a unique property of these open cellulose films. It shows that the dimensions of the imaged features should be considered before dismissing the lateral dimensions as tip exaggeration—a dismissal often prevalent in literature [38–40].

3.3. Wetting and drying of the open cellulose films

When immersed in water, fibre swells because water penetrates into the amorphous areas of the fibre matrix. When the swollen fibre is dried, irreversible changes take place and the dried fibre does not swell to the same extent as it did before the drying. Some flexibility of the fibre is lost and the resulting fibre network after papermaking has inferior strength properties [28,29]. The described phenomenon—often called 'hornification' in the jargon of paper technology—is the main reason behind the declined strength of recycled paper, since recycling always involves rewetting of fibre and subsequent drying. Its fundamental nature is not yet understood. Keeping in mind the differences between native cellulose and nanosized cellulose patches on silicon, we wanted to examine, whether any distinct morphological changes were to be seen if the patches were swollen in water and dried afterwards. No direct link to hornification is attempted, but if the results proved auspicious, they can point us to further experiments which, together with additional analytical techniques, are able to yield information about the supramolecular structure and rearrangements of amorphous cellulose.

The idea in the wetting/drying experiments with open cellulose films was to immerse the surface totally in water, evaporate the excess (visible) water fast in 80 °C, and follow the drying by AFM measurements after gradual heating steps in 110 °C which is the standard temperature to dry the fibre in laboratory conditions. The immersion was performed by placing droplets of water on the wafer so that it

Table 1
Volume quantification from parallel experiments

Sample number	1	2	3	4
Cellulose volume ($nm^3/\mu m^2$)	2.806×10^5	2.792×10^5	2.807×10^5	2.855×10^5

Four cellulose films prepared from 20 mg/l TMSC solution, hydrolysed in 2 M HCl (g) for 2 min. 1 μm^2 AFM scans.

Table 2
Coverage and volume quantification for the 1 μm^2 AFM images of Fig. 2

Spin coating concentration (mg/l)	Corresponding figure	Cellulose coverage (%)	Cellulose volume ($nm^3/\mu m^2$)
10,000	2(a)	100	180×10^5
50	2(b)	58	3.6×10^5
20	2(c)	43	2.8×10^5
10	2(d)	35	0.6×10^5

was fully covered with water. In that way we could be sure that no cellulose was lost during the immersion, although the experiments with our closed films suggest that water does not detach cellulose, once deposited on the silicon wafer [18]. Fig. 5 shows the visual results of this procedure. Coverage has been determined from histograms as in Fig. 1, and volume is given by Eq. (1). Fig. 5(a) is the untreated open cellulose film spin coated from 20 mg/l TMSC solution and hydrolysed for 2 min in 2 M HCl (g) (similar to Fig. 2(c)). The sample in Fig. 5(a) was immersed in water for 15 min, after which the excess water (visible to naked eye) was dried in 80 °C (ca. 3 min) and the sample was immediately cooled down to room temperature. The resulting AFM image from this sample is presented in Fig. 5(b). Noticeable swelling has taken place. Also, the cellulose coverage has decreased. After 15 min of drying in 110 °C, the width of the patches decreases considerably (Fig. 5(c)) and after further 45 min in 110 °C (Fig. 5(d)), slight decrease in width and some heightening takes place (Fig. 5(d)).

A straightforward qualitative observation is the presence of inflated regions in the patches of the partially dried cellulose (Fig. 5(c)). Clearly, there are regions in the patches where water prefers to stay longer. These regions are likely to be the sites for inter-chain hydrogen bonding. This is consistent with the model proposed for amorphous cellulose: randomly distributed amorphous domains are partly interacted by intermolecular hydrogen bonds [41]. The direct visualization of this is an encouraging result. More experiments with different drying and wetting techniques—vapour vs. water immersion, for instance—are bound to give us more direct morphological evidence on the arrangement of amorphous cellulose.

Table 3 gathers the quantified data from Fig. 5. Coverage and apparent volume were determined from the height histograms and Eq. (1) (Section 2), patch length was calculated by Scanning Probe Image Processor (image metrology), the patch height was taken from manual analysis of 10 height scans (ca. 80 heights) and patch width from manual cross sectional analysis of 30 patches in each image. The tip exaggeration on width diameter was evaluated for tips of 5 nm (min) and 10 nm (max) radii of curvature as in Section 3.2. These degrees of exaggeration were used to calculate the respective exaggeration in the area of cross sections, thus yielding the corrected volume (average of the exaggeration by 5 and 10 nm tips) and the corresponding error.

It is the error from varying tip radii that renders the volume determination inaccurate when the width becomes relatively small compared with the height. The extent of exaggeration to the lateral dimensions can always be corrected for parabola-like cross sections. Yet when the width/height ratio of the parabola becomes too large, the tip error inflates considerably. One can conclude from Table 3 that, as a rule of thumb, when the measured width/height ratio of a parabola-like cross section is around 15 or more (as in Fig. 5(a) and (b)) the volume quantification by Eq. (1) has a reasonable error ($<2\%$). Once the width/height ratio of a cross section descends below 10 (as in Fig. 5(d)), the error ($>30\%$) gets out of hand.

The overall pattern from Fig. 5 and Table 3 is clear: the patches swell during wetting and shrink as they are dried. From the wet state (Fig. 5(b)) to the dried state (Fig. 5(c) and (d)) only heating is applied, i.e. the change in volume is caused by the removal of water. This indicates that the cellulose patches are mostly amorphous since crystalline cellulose is largely impenetrable by water [7]. The volume from the ambient (Fig. 5(a)) to the dried state (Fig. 5(d)) stays constant or decreases slightly—regrettably the error of volume quantification with Fig. 5(d) results in slightly dubious interpretation. What is certain, however, is that the height of the patches doubles between ambient and wet state (Fig. 5(a) to (b)) and that the partially dried patches (Fig. 5(c)) contract in width and increase moderately in height (Fig. 5(d)). The volume does decrease from Fig. 5(c) to (d) (Table 3), meaning that drying is still taking place after the initial 15 min of drying. The morphology between the initial state (Fig. 5(a)) and the final dried state (Fig. 5(d)) is certainly different.

The 1×1 μm^2 scans of Fig. 5 can be misleading without a larger-size picture. We cannot be certain, for instance, if there is uneven migration of the cellulose chains during the water immersion (between Fig. 5(a) and (b)). This would mean that scans from different areas on the surface are not equally representative. Since the 1×1 μm^2 could never be performed at exactly the same place on the wafer, we performed larger scans. Fig. 6 provides 5×5 μm^2 scans of Fig. 5(a) (Fig. 6(a)) and Fig. 5(b) (Fig. 6(c)). The homogeneity of the layers is apparent in both cases. The homogeneity also signifies that the migration of cellulose chains during the soaked state (between Fig. 5(a) and (b)) is not a decisive factor in the morphological changes in Fig. 5, even though we cannot completely rule it out. Further evidence for the cellulose content's staying constant in the

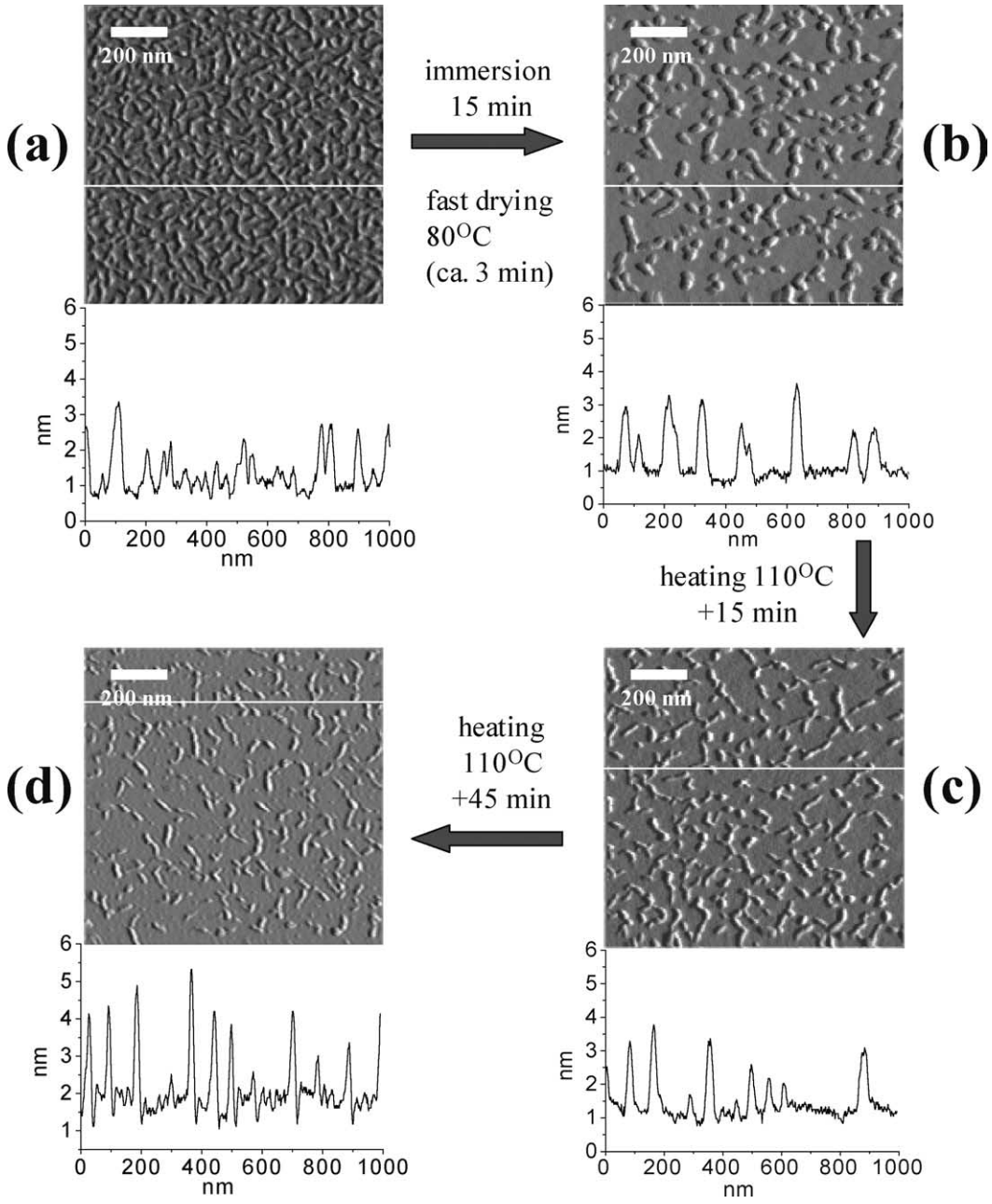

Fig. 5. $1 \times 1\ \mu m^2$ AFM images of wetting/drying scheme of an open cellulose film from 20 mg/l TMSC solution, hydrolysed to cellulose with 2 M HCl vapour for 2 min: (a) untreated open cellulose film in ambient conditions; (b) same film after immersion in water for 15 min and fast drying in 80 °C (until the water has visibly evaporated from the wafer); (c) same film after drying in 110 °C for 15 min; (d) same film after drying in 110 °C for further 45 min. All measurements were performed at room temperature. A representative height scan marked in the image is presented under each image.

patches from Fig. 5(a) to (d) appears when the corrected width is compared with the corrected coverage (Table 3): the width of the patches in Fig. 5(a) is roughly double to that of Fig. 5(d). The same applies for coverage, which would mean a similar amount of cellulose chains in Fig. 5(a) and (d), provided they are both devoid of water to a large extent. The coverage is actually a product of the length of the cellulose network and the average width. Consequently, the coverage divided by the average width is the same, and the length of the whole network should then be the same.

Fig. 6(b), on the other hand, is a unique image of an intermediate state between Fig. 6(a) and (c). It has been achieved by drying the soaked sample in a gentler temperature of 50 °C, instead of the normal 80 °C of fast drying between the Fig. 6(a) and (c) (and smaller scans of Fig. 5(a) to (b)). Large amounts of water still prevail on the surface, the higher regions rising up to 10 nm in height. The quantification of Fig. 6(b) is limited because of its exclusive nature, but it shows that, with carefully chosen parameters, the tapping mode

Table 3
Volume, coverage and volume/coverage ratio of the cellulose patches in 1 μm^2 AFM scans

Treatment	Ambient	Wetting–drying in 80 °C	110 °C + 15 min	110 °C + 45 min
Figure	5(a)	5(b)	5(c)	5(d)
Patches coverage (%)	43	35	31	30
Average patch length (nm)	[a]	64	54	53
Apparent volume (10^5 $nm^3/\mu m^2$)	2.8	4.4	4.0	3.6
Average patch width (nm)	20	31	18	15
Tip exaggeration on width diameter (nm)	1.5 ± 0.5	2.2 ± 0.2	3.0 ± 1.0	4.7 ± 1.7
Corrected patch width (nm)	18.5 ± 0.5	28.8 ± 0.2	15.0 ± 1.0	10.3 ± 1.7
Corrected volume (10^5 $nm^3/\mu m^2$)	2.65 ± 0.05	4.2 ± 0.1	3.4 ± 0.3	2.3 ± 0.7
Corrected coverage (%)	40 ± 1	33 ± 1	26 ± 2	21 ± 3
Average patch height (nm)	0.9 ± 0.1	1.8 ± 0.1	1.6 ± 0.1	1.9 ± 0.1

The wetting/drying scheme of Fig. 5.
[a] Impossible to determine because of extensive overlapping between the patches.

AFM can be stretched to image highly ambient states of cellulose films, similar to images of self-dewetting polymers [42].

Scheme 2 offers a schematic explanation of the possible events in Fig. 5, on the basis of data in Table 3. The cross sections in Scheme 2 represent the cross sections of an average cellulose patch in each Fig. 5 image. The lines depict cross sections of individual cellulose chains (7 Å × 3 Å) that are more or less arbitrarily arranged in accordance with the patches' amorphous nature. We have presumed that the number of the cellulose chains between ambient and wet state is the same (Fig. 5(a) and (b)). The important interpretation from Scheme 2 is that in the dried state (Scheme 2(d), corresponding to Fig. 5(d)), the cellulose chains are forced to form small regions with a higher degree of order. Moreover, the increased height of the dried patches suggests that the cellulose chains would arrange perpendicular to the silicon surface (Scheme 2(d), Fig. 5(d)), as opposed to the ambient state (Scheme 2(a), Fig. 5(a)) where the alignment would be more parallel to the substrate. The driving force behind this is probably the reduction of the surface area—the surface energy, thus—between the hydrophobic part of the patches (glucopyranose ring in cellulose) and the relatively hydrophilic silicon upon drying. The optimisation of surface energy is already taking place from the TMSC to the cellulose patches (Fig. 3(b) to (c)), but the morphology is still within the constraints of the original morphology of the TMSC film which is a closed network. Water immersion allows the cellulose patches to arrange on the substrate in thermodynamically the most favourable form. This is another observation that accentuates the difference between amorphous patches on silicon and natural cellulose. In the future, it would be interesting and more authentic to expand the surfaces so that the cellulose patches could be blended in with other materials from cell walls, such as lignin or hemicellulose. We are currently working on the issue and the results will be published later elsewhere.

We want to stress the conditional tense in these interpretations. The large error in the case of Fig. 5(d), uncertainty of the possible migration of cellulose in the soaked state, and the pilot nature of these experiments would leave us in a predicament if unambiguous conclusions were drawn.

However, this introduction is an indication that the open cellulose films can be exploited to draw conclusions about the supramolecular architecture of amorphous cellulose in a very small scale, provided that more experiments are conducted, and that more analytical techniques are incorporated. Especially additional analysis of the open films is absolutely vital, since it would reveal, among other things, whether any water has been trapped inside the dried cellulose or the amount of charged end groups which are vital in applying the Donnan theory to swelling [43]. Furthermore, experiments in varying pH-values would consider the polyelectrolyte nature of cellulose. The crystallinity of the cellulose patches is also important. In fact, even though we have presumed the patches be amorphous, it is based merely on an indication from the swelling of the patches, whereas the actual degree of crystallinity remains undetermined. The small size of the patches challenge the limitations of any instrumental technique, but it is surely surmountable.

4. Conclusions

Refining the previously published method of spin coating trimethylsilyl cellulose (TMSC) and hydrolysing it back to cellulose [17,18], we have managed to reproducibly prepare open nanosized films of cellulose on an untreated silicon substrate. Atomic Force Microscopy (AFM) revealed that, in the open films, cellulose arranges into patches which have lateral dimensions of roughly 20 × (50–100) nm and the height of 0.9 nm. The AFM histogram of the height distribution over the surface showed two distinct features which could be resolved to silicon and cellulose contributions by Gaussian peak fit. In addition, the volume of the cellulose patches could be quantified from the histograms with considerable accuracy. The lateral exaggeration by the

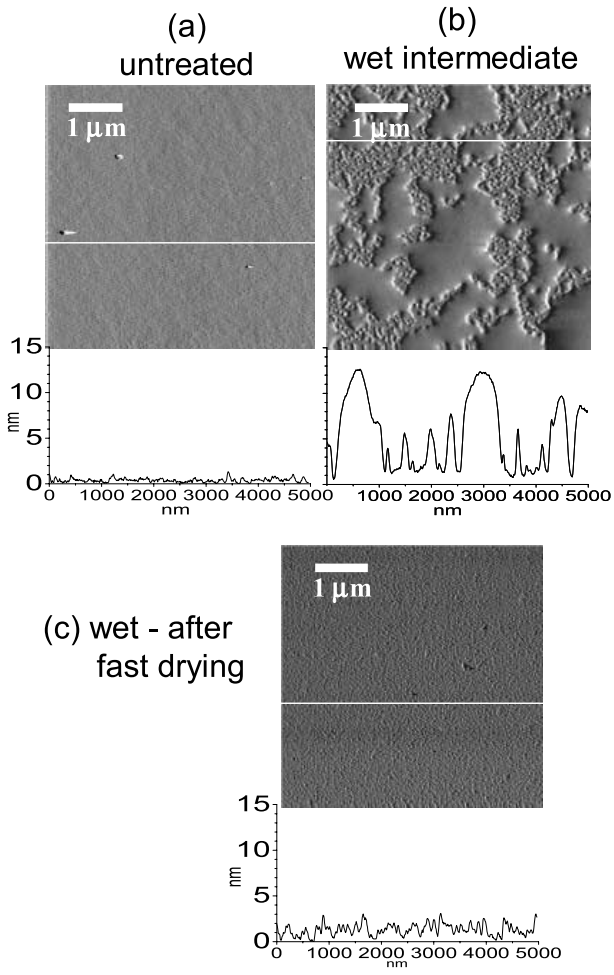

Fig. 6. $5\times5\ \mu m^2$ AFM images of wetting/drying scheme of an open cellulose film from 20 mg/l TMSC solution, hydrolysed to cellulose with 2 M HCl vapour for 2 min: (a) untreated open cellulose film in ambient conditions; (b) open cellulose film after immersion in water for 15 min and gentle drying in 50 °C (until the water has visibly evaporated from the wafer); (c) same film as in (a) after immersion in water for 15 min and fast drying in 80 °C (until the water has visibly evaporated from the wafer). All measurements were performed at room temperature. A representative height scan marked in the image is presented under each image. (a) and (b) are zoomed scans of Fig. 5(a) and (b), respectively.

AFM tip on the image was found to be around 6% with an error of $\pm2\%$. The small error arises because of the flatness of the cellulose patches. When the measured width/height ratio of parabola-like cross sections is around 15 or more the volume quantification has a reasonable error ($<2\%$). When the width/height ratio of a cross section descends below 10, the error ($>30\%$) gets out of hand.

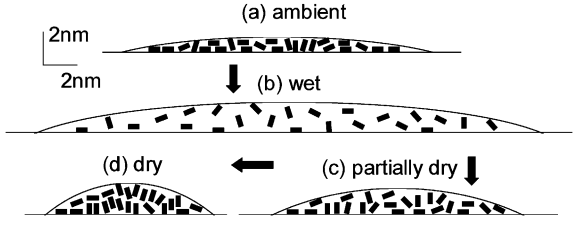

Scheme 2.

The open cellulose films and their availability for volume quantification were utilized by examining the behaviour of cellulose patches during wetting and drying with water. Expectedly, swelling was observed among wetting, and shrinking after drying. However, the morphology was not restored reversibly, which indicates that the open films are suitable for interpretation when investigating the supramolecular rearrangements of cellulose during wetting and subsequent drying. Other characterization techniques are necessary to fully take advantage of their potential, but our results show that the open films are a practical way to improve the otherwise vague knowledge of the amorphous rearrangements of cellulose.

Acknowledgements

The research described is part of the project 'Fibre raw material technology for sustainable production of paper and board'. This project is one of the activities of the Dutch Centre of Competence Paper and Board, and is supported by the Dutch Ministry of Economic Affairs. They are acknowledged for their financial support.

References

[1] Zugenmeier P. Prog Polym Sci 2001;26:1341.
[2] Nishiyama Y, Langan P, Chanzy H. J Am Chem Soc 2002;124:9074.
[3] Nishiyama Y, Sugiyama J, Chanzy H, Langan P. J Am Chem Soc 2003;125:14300.
[4] O'Sullivan AC. Cellulose 1997;4:173.
[5] Jakob HF, Tschegg SE, Fratzl P. Macromolecules 1996;29:8435.
[6] Zhou S, Tashiro K, Hongo T, Shirataki H, Yamane C, Ii T. Macromolecules 2001;34:1274.
[7] Klemm D, Philipp B, Heinze T, Heinze U, Wagenknecht W. Comprehensive cellulose chemistry. vol. 1. Weinheim: Wiley-VCH; 1998 [chapter 2].
[8] Coulier L, de Beer VHJ, van Veen JAR, Niemantsverdriet JW. Top Catal 2000;13:99.
[9] Loos J, Thüne PC, Niemantsverdriet JW, Lemstra PJ. Macromolecules 1999;32:8910.
[10] Schaub M, Wenz G, Wegner G, Stein A, Klemm D. Adv Mater 1993;5:919.
[11] Buchholz V, Wegner G, Stemme S, Ödberg L. Adv Mater 1996;8:399.
[12] Gunnars S, Wågberg L, Cohen Stuart MA. Cellulose 2002;9:239.
[13] Edgar CD, Gray DG. Cellulose 2003;10:299.
[14] Geffroy C, Labeau MP, Wong K, Cabane B, Cohen Stuart MA. Colloids Surf 2000;172:47.
[15] Rojas OJ, Ernstsson M, Neuman RD, Claesson PM. J Phys Chem B 2000;104:10032.
[16] Österberg M. J Colloids Interf Sci 2000;229:620.
[17] Kontturi E, Thüne PC, Niemantsverdriet JW. Polymer 2003;44:3621.
[18] Kontturi E, Thüne PC, Niemantsverdriet JW. Langmuir 2003;19:5735.
[19] Sukanek PC. J Imaging Technol 1985;11:184.
[20] Lee S-S, Lee K-B, Hong J-D. Langmuir 2003;19:7592.
[21] Yoon J, Ree M, Hwang Y, Lee SW, Lee B, Kim J-S, et al. Langmuir 2004;20:544.

[22] Niemantsverdriet JW, Engelen AFP, de Jong AM, Wieldraaijer W, Kramer G. J Appl Surf Sci 1999;144–145:366.
[23] Sheiko SS, Möller M. Chem Rev 2001;101:4099.
[24] Kiriy A, Gorodyska G, Minko S, Tsitsilianis C, Jaeger W, Stamm M. J Am Chem Soc 2003;125:11202.
[25] Sheiko SS, da Silva M, Shirvaniants D, LaRue I, Prokhorova S, Moeller M, et al. J Am Chem Soc 2003;125:6725.
[26] Sheiko SS, Prokhorova SA, Beers KL, Matyjaszewski K, Potemkin II, Khokhlov AR, et al. Macromolecules 2001;34:8354.
[27] Kasai W, Kondo T. Macromol Biosci 2004;4:17.
[28] Wistara N, Young R. Cellulose 1999;6:291.
[29] Maloney TC, Paulapuro H. J Pulp Paper Sci 1999;25:430.
[30] Fält S, Wågberg L, Vesterlind E-L. Langmuir 2003;19:7895.
[31] McCormick CL, Callais PA, Hutchison Jr BH. Macromolecules 1985; 18:2394.
[32] Klemm D, Philipp B, Heinze T, Heinze U, Wagenknecht W. Comprehensive cellulose chemistry. vol. 2. Weinheim: Wiley-VCH; 1998. p. 367.
[33] San Paulo A, García R. Biophys J 2000;78:1599.
[34] García R, San Paulo A. Phys Rev B 1999;60(4961):18.
[35] Paakkari T, Serimaa R, Fink H-P. Acta Polym 1989;40:731.
[36] Mazeau K, Heux L. J Phys Chem B 2003;107:2394.
[37] Alén R. Structure and chemical composition of wood. In: Stenius P, editor. Forest products chemistry. Helsinki: Fapet Oy; 2000. p. 35.
[38] Spencer ND, Jarvis SP. In: Moore JH, Spencer ND, editors. Scanning probe microscopies. Encyclopedia of chemical physics and physical chemistry, vol. 2. Bristol and Philadelphia: IoP Publishing; 2001. p. 1467–515.
[39] Niemantsverdriet JW. Spectroscopy in catalysis. 2nd ed. Weinheim: Wiley-VCH; 2000 [chapter 7].
[40] Schneider M, Brinkmann M, Möhwald H. Macromolecules 2003;36: 9510.
[41] Kondo T, Sawatari C. Polymer 1996;37:393.
[42] Sheiko S, Lermann E, Möller M. Langmuir 1996;12:4015.
[43] Grignon J, Scallan AM. J Appl Polym Sci 1980;25:2829.